doi: 10.3304/JMES.2017.002

Journal of Mediterranean Earth Sciences 9 (2017), 19-28

Journal of Mediterranean Earth Sciences

Activity concentration and spatial distribution of radon in beach sands of Gaza Strip, Palestine

Khalid Fathi Ubeid [a,*], Khaled Ahmed Ramadan [2]

[a] *Department of Geology, Faculty of Science, Al Azhar University - Gaza, P.O. Box 1277, Gaza Strip, Palestine*
[b] *Department of Physics, Faculty of Science, Al Azhar University - Gaza, P.O. Box 1277, Gaza Strip, Palestine*
[*] *Corresponding author:khubeid@hotmail.com*

ABSTRACT - Sand beach contamination by radon has been investigated along the beach of Gaza Strip, Palestine. Around forty samples of surface beach sands have been selected along the study area, then analyzed in the laboratory to find the grain-size distribution and radon activity concentration. The results showed grain-size fining towards the north direction, and high level radon activity in Gaza and North Governorates, both located in the northern side of the study area. These results suggest positive correlation between the grain-size of the sediments and radon concentration, and radon activity depending on black fine-grained sediments carried from Nile delta by longshore currents generated by approaching breaking waves. On the other hand, the slightly increasing in concentration levels were observed around the wastewater pumping stations which discharge in the beach. The annual effective dose (AED) in these governorates were above the standard international limit, whereas the AED of the radon in the remaining governorates in the Gaza Strip were below the standard international limit.

Keywords: Beach sand; Grain-size distribution; radon; Pollution; Gaza Strip; Palestine.

Submitted: 21 May 2017 - Accepted: 30 July 2017

1. INTRODUCTION

Naturally occurring radon (^{222}Rn; half-life = 3.82 days) that originates within the earth and is transported into indoor air in amounts large enough to constitute a health hazard has been a matter of concern around the world for several years. As a noble gas, radon is chemically inert and thus does not interact with bodily tissues. However, the inhalation of radon and thoron (^{220}Rn; half-life = 56 s) progeny, particularly the short-lived decay products (^{218}Po, ^{214}Pb, ^{216}Po, ^{212}Pb) can result in their deposition on respiratory tract tissues. Subsequent alpha decays may damage cells near the deposition sites, contributing to an increased risk of lung cancer (UNSCEAR, 1988; Katheren, 1998; USEPA, 2003; Hassan et al., 2009; Darby et al., 2004; Lubin et al., 2004; Krewski et al., 2005).

Radon emanates and diffuses from rocks/soils and trends to concentrate in pore spaces, its atoms have enough kinetic energy to reach the pore volume. It is released from the upper layers of rock and sediments with an average of 10% of radon formed in the soil being released in air. Radon migration can be described by two mechanisms, diffusion and advection flows. Its emanation is affected by many factors, such as grain-sizes, moisture content, porosity, permeability, position of radium (Ra) atoms in grains, etc. (e.g. Nazaroff, 1992; Markkanen and Arvela, 1992; Shweikani et al., 1995; Menetrez and Mosley, 1996; Sundal et al., 2004; Barillon et al., 2005; Immé et al., 2014).

The aim of this work is to assess the activity concentration levels of radon in the marine surface sands along the beach of Gaza Strip, Palestine, and to test a possible correlation between the concentration levels and the grain-size distribution of the sands.

2. MATERIALS AND METHODS

2.1. The Study area

The coastline of Palestine is broadly concave, generally trending NNE-SSW (Fig. 1A). It lies between two parallel lineaments. The eastern (onshore) lineament is an escarpment that locally is steeper than 45 degrees and rises as high as +50 m above mean sea level (MSL). Adjoining the coastline are coastal plain on the land and the continental shelf beneath the ocean. Both areas contain broadly curved subparallel sand ridges that are similar to each other. Smaller interruptions are provided by river valleys and by a ridge bifurcations.

The Gaza Strip is situated in the southwestern part of Palestine and southeast coast plain of the Mediterranean

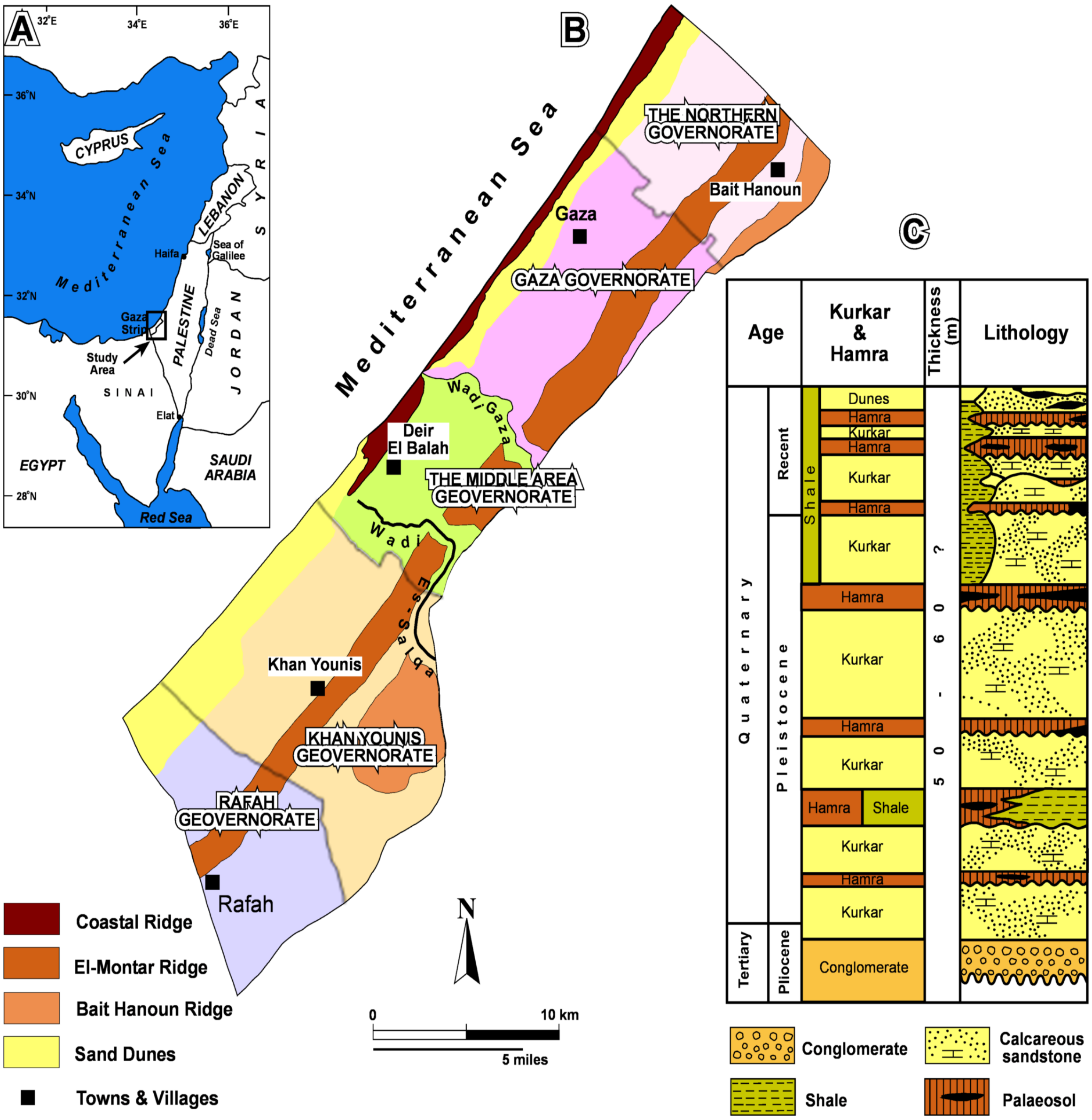

Fig. 1 - (A) Location map of the study area. (B) The kurkar ridges along the Gaza Strip (after Ubeid, 2010). (C) The lithology of Plio-Pleistocene of kurkar and hamra alternations (Gaza Formation) (after Abed and Al Weshahy, 1999).

Sea (Fig. 1A). The topography of Gaza Strip is defined by three ridges. The coastal ridge is up to 50 m above MSL, it extends up to the current coastline in the west; in the other hand, the Al-Montar and the Beit Hanoun ridges lay at the middle and the east of Gaza Strip (Fig. 1B). The three ridges consist of marine and continental calcareous sandstones which locally named as kurkar, and intercalated by red sandy loam soils locally called hamra (Fig. 1C). The ridges are separated by deep depressions (20-40 m above MSL) with alluvial deposits (Ubeid, 2010).

The coastal zone of Gaza Strip is 45 km long, while the width of the Strip is between 6 to 12 km covering an area of 365 km^2. The coastal zone is defined as a band of water and land along the marine shoreline where different activities interact with each other. It includes the sand dunes in the south and north, the coastal cliffs (exposed kurkar ridges) in the middle to north, the non-urban areas, and part of Gaza valley 'Wadi Gaza'. The land of the coastal zone covers about 74 km^2 of which 2.7 km^2 are beaches (Ubeid and Albatta, 2014).

The coastline has a straight and sandy shore. The near-coast continental shelf slopes down with a gradient of 1:100. The coastal shelf of Gaza is 28 km wide in the south of Gaza (i.e. to the 100 m depth line) and 14 km in the north. Beyond the 100 m depth line, the sea bottom drops quickly. The sea bottom sediments mainly consist of sand 25 m depth and there are some muddy places near the Wadi Gaza. Down to a depth of 100 m, the seabed is irregular with rocky grounds (Soghreah, 1996).

The sand dunes which cover large areas along the beach particularly in the southern part and the kurkar (hard sandstones) that crop out along the beach have been used extensively for construction since ancient times. Moreover, the beach of the Gaza Strip is considered a favorable recreation place for people. The total population of the Gaza Strip was about 2 million inhabitants.

Along the coast of Gaza Strip around eight sewage stations are observed in addition to Wadi Gaza, which are pumping poorly treated or untreated sewage into the seawater. One of sewage stations is located in North; three stations in Gaza; two stations in the Middle; one in Khan Younis; and one in Rafah Governorate (Fig. 2). The sewage is either disposed near the seashore or few meters inside the seawater.

2.2. Field Procedure

The field survey was carried out along the Gaza strip field from south to north direction. Forty observation sites were selected along the Gaza Strip beach as indicated in Figure 2, and located by global position satellite (GPS) technology (Tab. 1). At least 3 kg of representative sand samples were collected from the uppermost centimeters of each site.

2.3. Laboratory analysis

This study determined particle sizes by sieving method. Initially, the samples were dried at 105 C° for 24 hours in an oven. After drying of the sediment samples, sieving method was performed by sieve shaker to classify the particle sands of each sample, by using eight sieves (2000, 1180, 600, 425, 300, 212, 150, 63 µm). The initial weight of each sand sample was kept constant at 100 g, and the duration of shaking was about 15 minutes for each sample. At the end of the shaking time, the retained weight of sediment in each sieve was determined separately. The results of grain-size analysis are generally expressed in terms of the percentage of the total weight of sample that passed through the eight sieves.

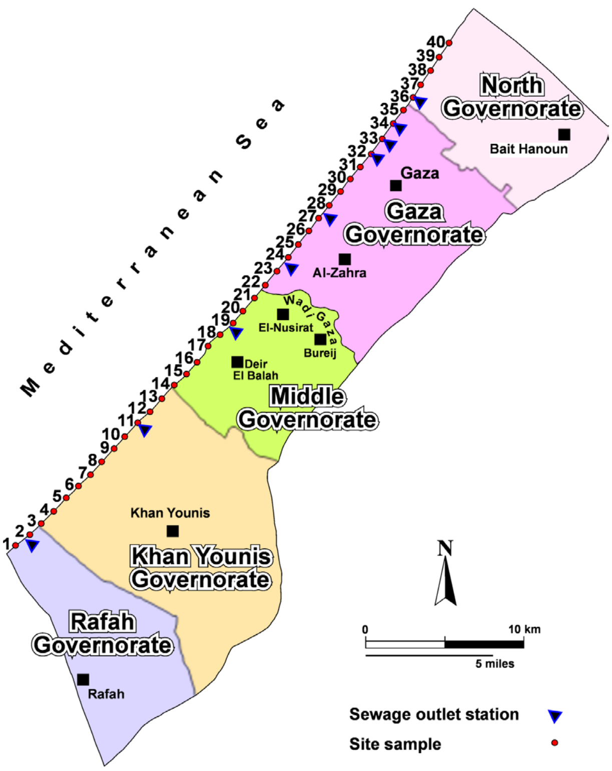

Fig. 2 - Location of the observation sites in the study area.

Site no.	Location	N	E
1	Rafah Governorate	31.32391	34.21988
2		31.33083	34.22821
3	Khan Younis Governorate	31.33614	34.23484
4		31.34251	34.24188
5		31.34904	34.24970
6		31.35542	34.25704
7		31.30158	34.26453
8		31.36760	34.27181
9		31.37460	34.27889
10		31.38112	34.28522
11		31.38794	34.29314
12		31.39421	34.30023
13		31.40022	34.30847
14	Middle Governorate	31.40683	34.31593
15		31.41277	34.32331
16		31.41854	34.33003
17		31.42572	34.33814
18		31.43238	34.34486
19		31.44004	34.35241
20		31.44606	34.35827
21		31.45295	34.36492
22	Gaza Governorate	31.45996	34.37160
23		31.46672	34.37854
24		31.47365	34.38515
25		31.48078	34.39192
26		31.48761	34.39853
27		31.54945	34.40548
28		31.50110	34.41213
29		31.50832	34.41830
30		31.51529	34.42458
31		31.52256	34.42965
32		31.52871	34.43711
33		31.53682	34.44464
34		31.54345	34.46122
35		31.55054	34.45734
36	North Governorate	31.55796	34.46327
37		31.56591	34.46973
38		31.57277	34.47496
39		31.58034	34.48088
40		31.58749	34.48629

Tab. 1 - The coordinates of the sampling sites.

After that, the data were processed using GRADISTAT software (Blott and Pye, 2001) to obtain the grain-size distribution (Tab. 2). In this software the linear interpolation is used to calculate statistical parameters and for describing the grain parameters (Folk and Ward, 1957).

Sample no.	Location	Coarse sand (%)	Medium sand (%)	Fine sand (%)	V. Fine sand (%)	Description	
						Mean	Sorting
1	Rafah Governorate	26.2	67.9	5.6	0.3	Medium sand	Moderately well sorted
2		7.0	71.0	20.6	1.4	Medium sand	Moderately well sorted
3	Khan Younis Governorate	4.9	76.2	18.5	0.5	Medium sand	Moderately well sorted
4		4.0	65.3	30.0	0.7	Medium sand	Moderately well sorted
5		6.2	76.8	16.9	0.1	Medium sand	Moderately well sorted
6		29.5	61.9	8.5	0.1	Medium sand	Moderately well sorted
7		9.4	76.5	13.5	0.6	Medium sand	Moderately well sorted
8		9.2	74.1	16.5	0.2	Medium sand	Moderately well sorted
9		11.3	68.8	19.6	0.3	Medium sand	Moderately well sorted
10		7.5	67.9	24.2	0.4	Medium sand	Moderately well sorted
11		16.1	63.6	19.8	0.6	Medium sand	Moderately well sorted
12		7.5	73.0	19.0	0.5	Medium sand	Moderately well sorted
13		3.9	61.6	29.7	4.8	Medium sand	Moderately well sorted
14	Middle Governorate	7.4	76.0	16.5	0.1	Medium sand	Moderately well sorted
15		5.8	77.6	16.4	0.3	Medium sand	Moderately well sorted
16		4.3	40.1	51.6	4.0	Fine Sand	Moderately well sorted
17		9.5	63.1	26.3	1.2	Medium sand	Moderately well sorted
18		2.5	50.0	43.3	4.2	Medium sand	Moderately well sorted
19		3.6	58.5	35.4	2.5	Medium sand	Moderately well sorted
20		8.1	64.6	25.8	1.6	Medium sand	Moderately well sorted
21		4.6	64.5	29.1	1.8	Medium sand	Moderately well sorted
22	Gaza Governorate	13.0	68.2	17.2	1.6	Medium sand	Moderately well sorted
23		1.7	48.9	47.3	2.1	Medium sand	Moderately well sorted
24		4.6	61.5	31.1	2.7	Medium sand	Moderately well sorted
25		1.9	59.1	36.8	2.1	Medium sand	Moderately well sorted
26		4.2	63.5	31.2	1.1	Medium sand	Moderately well sorted
27		7.2	65.5	25.4	2.0	Medium sand	Moderately well sorted
28		1.2	51.4	45.1	2.3	Medium sand	Moderately well sorted
29		3.5	57.1	37.0	2.5	Medium sand	Moderately well sorted
30		0.7	39.6	55.7	4.1	Fine Sand	Moderately well sorted
31		0.4	25.2	69.9	4.5	Fine Sand	Moderately well sorted
32		0.2	9.0	68.7	22.1	Fine Sand	Moderately well sorted
33		2.5	48.1	40.6	8.8	Fine Sand	Moderately well sorted
34		10.2	74.6	15.0	0.3	Medium sand	Moderately well sorted
35		2.0	43.4	45.2	9.4	Fine Sand	Moderately well sorted
36	North Governorate	13.3	77.7	8.3	0.7	Medium sand	Moderately well sorted
37		11.8	82.1	6.1	0.0	Medium sand	Moderately well sorted
38		10.2	77.2	12.3	0.3	Medium sand	Moderately well sorted
39		3.4	65.6	30.5	0.5	Medium sand	Moderately well sorted
40		2.4	41.9	51.9	3.9	Fine Sand	Moderately well sorted

Tab. 2 - The grain size distributions of beach sand samples.

2.4. The activity measurements

In this study, the activity concentrations of the samples were measured using cup technique and solid-state nuclear track detectors CR-39 for monitoring radon in this study. The detectors were cut in small pieces (usually 1cmx2cm) and fixed at the top of the plastic container (3 liters, diameter of 14 cm), 300 cm^3 of the sediment sample were put at the bottom of container, the detector was exposed to air containing radon emanated from the sediment for a time period of 95 day. At the end of the exposure time, the CR-39 films were chemically etched using a 6M solution of NaOH, at a temperature of 70 ^oC, for about 5 hours. The detectors were washed with distilled water and left to dry. Each detector was counted visually using an optical microscope through the area within 3 mm^2 in 4 distinct regions, and the average number of tracks/mm^2 was determined from the measured average track densities on the CR-39, with detector sensitivity 0.41 Bq/m^3 per tracks cm^{-2} month^{-1}. Radon calculations in this study were carried out using the following equations:

$$E = \frac{k\rho}{A}\left[\frac{\lambda V}{T_{eff}}\right] \quad (1), \quad C_{Rn} = k\frac{\rho}{T_{eff}} \quad (2), \quad C_{Ra} = k\frac{\rho V}{MT_{eff}}, \quad (3)$$

where, E is radon exhalation rate (Bq m^{-2} h^{-1}), C_{Rn} is the radon concentration (Bq/m^3), C_{Ra} is the effective radium content (Bq/kg), ρ is the track density (tracks / cm^2), k is the detector sensitivity (Bq m^{-3}/tracks cm^{-2} h^{-1}), λ is the decay constant (λ= 7.56 x 10^{-3} h^{-1}) , V is the free volume of the container (cm^3), A is the area of the sample (cm^2), M is the mass of the sample (kg), and T_{eff} is the effective exposure time (Baykara and Dogru, 2006; Baykara et al., 2005; Sroor et al., 2001).

UNSCEAR (2000) report noted the difference in radon doses and recommended a radon effective dose conversion factor (of 9 nSv per (Bq h m^{-3}). Then the annual effective dose (AED) was calculated from radon concentrations. Assuming an indoor occupancy factor of 80% (T = 7000 hours per year), an equilibrium factor (ε) of 0.4 (Chen, 2005), using the mentioned UNSCEAR recommendation, the effective dose for one year radon exposure is calculated using the relation:

$$AED = \varepsilon f_{Rn} T C_{Rn} \quad (4)$$

where ε is the equilibrium factor (= 0.4), f_{Rn} is the conversion factor (= 9 nSv / (Bq h m^{-3})), T is the time spent indoors per year (= 7000 hours), and C_{Rn} is the radon concentration (Guo and Cheng, 2005).

3. RESULTS AND DISCUSSION

3.1. Sand beach characteristics

The sand beach of the Gaza Strip is characterized by a light yellow color. From the results of mechanical analysis of surface sands it was observed that the samples are composed of high percentage of quartz, with light color to transparence and sugary-like, in addition to this, around 1% of accessory minerals with dark color. Most of samples contain coarse- to very coarse-sized shell fragments of pelecypods and gastropods that represent around 1% of the total weight.

The grain size parameters of sands from 40 observation sites along the beach of Gaza Strip are shown in Table 2. The analysis of surface sand samples shows that the predominant grain size of the samples are medium-sized, excluding sample no. 16, 30, 31, 32, 33, 35, and 40 that are fine-grained. These sites are located in northern part of Gaza Strip indicating that the grain size is finer toward the north (Fig. 3). This composition is probably the result of sediment transport processes, sedimentation in the different sectors of the beach, variable extent of exposure to hydrodynamic agents and longshore gradients of wave energy.

All the samples had moderately well sorting (Tab. 2). This could be referred to sea-wave abrasion that has improved their sands' sorting. Well-sorted medium sand is mainly associated with the effects of the marine, fluvial, and eolian selectiveness that produces it due to the hydraulic action of waves in beach sedimentary environments and wind in dune areas (Carranza-Edwards, 2001; Carranza-Edwards et al., 2009; Ubeid and Albatta, 2014).

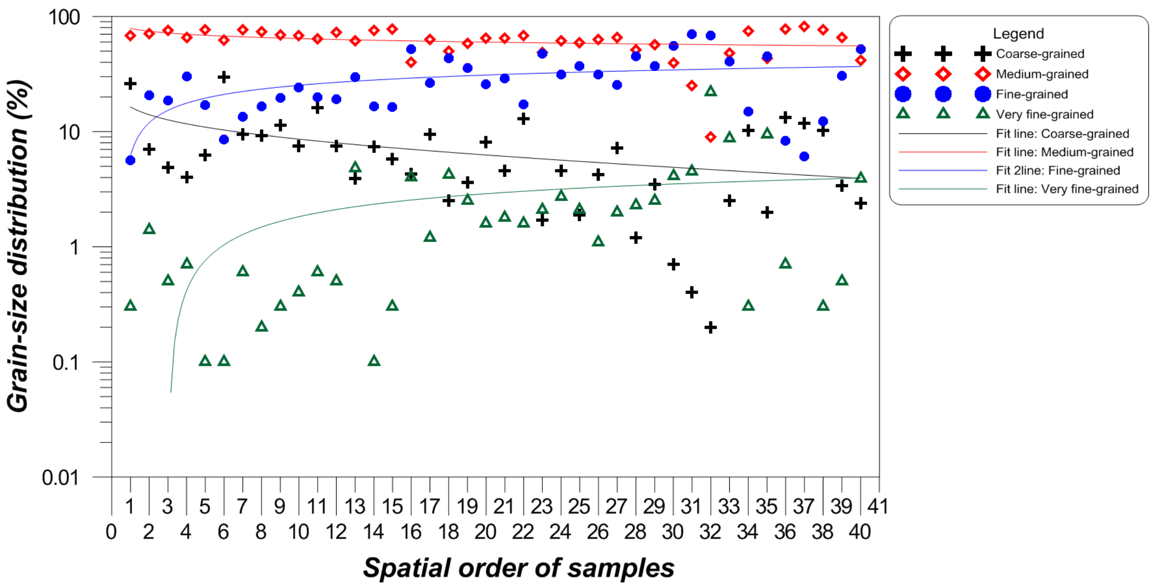

Fig. 3 - Correlation of grain-size distribution along the beach of Gaza Strip.

Samples no.	Location	E (mBq/m^2 h)	C_{Rn} (Bq/m^3)	C_{Ra} (Bq/kg)	Dose (mSv/y)
1	Rafah Governorate	123.5	122.4	0.70	3.1
2		223.1	221.2	1.24	5.6
3	Khan Younis Governorate	151.6	150.3	0.84	3.8
4		101.8	100.9	0.56	2.5
5		120.2	119.2	0.66	3.0
6		167.9	166.4	0.92	4.2
7		200.4	198.6	1.09	5.0
8		128.9	127.8	0.70	3.2
9		179.8	178.2	0.98	4.5
10		170.0	168.6	0.95	4.2
11		154.9	153.5	0.85	3.9
12		120.2	119.2	0.65	3.0
13		146.2	145.0	0.81	3.7
14	Middle Governorate	143.0	141.7	0.77	3.6
15		96.4	95.6	0.53	2.4
16		113.7	112.7	0.62	2.8
17		122.4	121.3	0.67	3.1
18		134.3	133.1	0.73	3.4
19		166.8	165.4	0.89	4.2
20		161.4	160.0	0.89	4.0
21		149.5	148.2	0.82	3.7
22	Gaza Governorate	265.3	263.1	1.48	6.6
23		213.4	211.5	1.22	5.3
24		214.4	212.6	1.21	5.4
25		167.9	166.4	0.92	4.2
26		240.4	238.4	1.33	6.0
27		257.8	255.6	1.41	6.4
28		159.2	157.8	0.88	4.0
29		261.0	258.8	1.46	6.5
30		421.3	417.7	2.52	10.5
31		220.9	219.0	1.41	5.5
32		327.1	324.3	1.97	8.2
33		150.5	149.3	0.82	3.8
34		1279.1	1268.2	6.97	32.0
35		306.5	303.9	1.82	7.7
36	North Governorate	228.5	226.6	1.26	5.7
37		1202.1	1191.8	6.58	30.0
38		1161.0	1151.0	6.33	29.0
39		1464.1	1451.5	8.46	36.6
40		229.6	227.6	1.31	5.7

Tab. 3 - Activity concentration of radon in Gaza Strip beach surface sands.

3.2. The activity concentrations

The results of activity measurements for identified radionuclides of the radon in the beach surface sands of the Gaza Strip are presented in Table 3. These results were consistent with some studies in different regions (e.g.; Rahman et al., 2007; Saad et al., 2013) (Tab. 4). The activity concentration are also depicted in Figure 4 with the sampling locations in the spatial order.

Radium activity in sand samples range from 0.56 to 8.46 Bq/kg, with a mean value of 1.66 Bq/kg and standard deviation 1.90. The highest values of the radium activity concentration were observed in the Gaza and North Governorates (0.82-8.46 Bq/kg). Concentrations start to rise from the south direction of Gaza Governorate until they reach their highest values in North Governorate 1.26-8.46 Bq/kg) (Tab. 3 and Fig. 4). In Gaza and North Governorates the concentration values were (0.82-6.97) and (1.26-8.46) Bq/kg, with average values of 1.82 and 4.79 Bq/kg, and standard deviation 1.55 and 3.3, respectively.

It is remarkable that the AED values in the Gaza and North Governorates in Gaza Strip are above the standard limits of the National Council on Radiation Protection and Measurements (1-5 mSv/y) (NCRP, 1978).

The remaining governorates, Middle, Khan Younis, and Rafah in Gaza Strip have little variation and low activity concentrations. The concentration values in these governorates range between (0.53-0.89), (0.56-1.09), and (0.70-1.24) Bq/kg, with average values 0.74, 0.82, and 0.97 Bq/kg, and standard deviation 0.13, 0.16, and 0.38, respectively (Tab. 5).

The AED in the sands beach of Middle, Khan Younis and Rafah Governorates are below the standard limits of the National Council on Radiation Protection and Measurements and United Nations Scientific Committee on the Effects of Atomic Radiation (NCRP, 1987; UNSCEAR, 2000).

Higher radon concentration at Gaza and North Governorates and in some observation sites (number 2 and 7) in Rafah and Khan Younis Governorates could be possibly associated with large volumes of untreated wastewater discharges from close pumping stations and to Wadi Gaza which also releases large amount of sewage into the beach (Fig. 2). It worth to mentioning that, these locations are close to agricultural lands, and the wastewater which is transported to the beach through the drainages and runoff carries fertilizers remains and painting materials disposal, which likely contain high amount of radium (Scholten and Timmermans, 1996). Particularly relevant, these drainages and runoff increase

Region	Type sample	E (mBq/m^2 h)	C_{Rn} (Bq/m^3)	C_{Ra} (Bq/kg)	Reference
Palestine (Gaza Strip)	Sand	96-1464	96-1452	0.56-8	This study
Palestine (Nablus)	Sand	38-121	21-68	0.22-0.73	Shoqwara et al. (2013)
Pakistan	Soil	263-331	101-143	-	Rahman et al. (2007)
Libya (Benghazi)	Soil	31-460	31- 469	1.50-23	Saad et al. (2013)

Tab. 4 - The radon concentrations of the sediments from different regions.

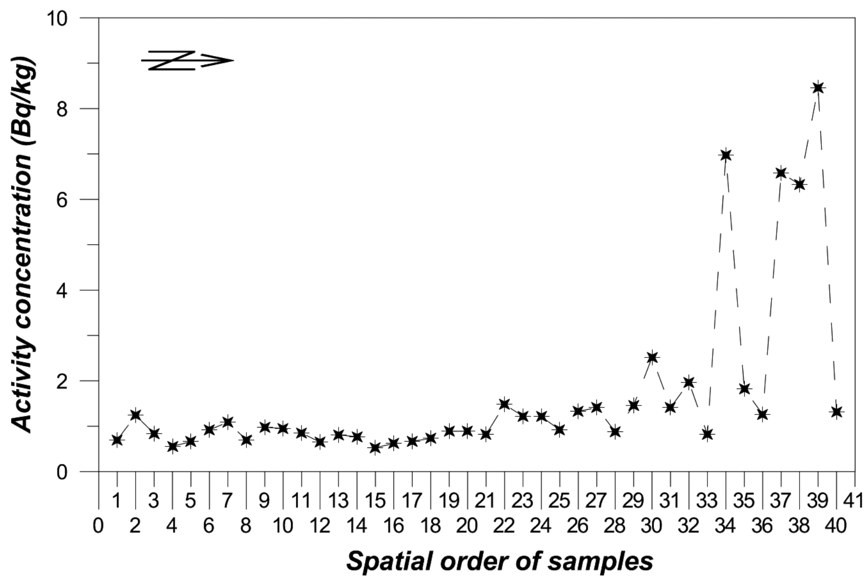

Fig. 4 - The activity concentration of radon in beach surface sands in site locations of the study area. At the x-axis locations are depicted the spatial order (number 1 is the location close to Rafah border at the south direction and number 40 the last site in the north direction).

Location	Statistics	E (mBq/m^2 h)	C_{Rn} (Bq/m^3)	C_{Ra} (Bq/kg)	Dose (mSv/y)
Rafah Governorate	Min.	123.5	122.4	0.70	3.1
	Max.	223.1	221.2	1.24	5.6
	Average	173.3	171.8	0.97	4.4
	St. Dev.	70.4	69.9	0.38	1.8
Khan Younis Governorate	Min.	101.8	100.9	0.56	2.5
	Max.	200.4	198.6	1.09	5.0
	Average	149.3	148.0	0.82	3.7
	St. Dev.	29.5	29.3	0.16	0.7
Middle Governorate	Min.	96.4	95.6	0.53	2.4
	Max.	166.8	165.4	0.89	4.2
	Average	135.9	134.8	0.74	3.4
	St. Dev.	24.1	23.9	0.13	0.6
Gaza Governorate	Min.	150.5	149.3	0.82	3.8
	Max.	1279.1	1268.2	6.97	32.0
	Average	320.3	317.6	1.82	8.0
	St. Dev.	285.2	282.7	1.55	7.1
North Governorate	Min.	228.5	226.6	1.26	5.7
	Max.	1464.1	1451.5	8.46	36.6
	Average	857.1	849.7	4.79	21.4
	St. Dev.	585.0	580.0	3.30	14.6
Total area	Min.	96.4	95.6	0.56	2.4
	Max.	1464.1	1451.5	8.46	36.6
	Average	296.2	293.6	1.66	7.4
	St. Dev.	339.6	336.7	1.90	8.5

Tab. 5 - Statistical analysis of activity concentration in surface sand samples in the study area.

in Northern area due rain regime which increase from SW to NW in Gaza Strip (Aish et al., 2009).

Additionally, the high activity concentration values in Gaza and North Governorates can be well explained by the observation that these areas have relatively high percentage of fine-grained black sediments. The grain-size analysis results show that the grains are fining towards north direction, and contain relatively high percentage of fine-grained black sediments in northern governorates comparing with middle and southern governorates (Shweikani et al., 1995; Filippidis et al., 1997; Kannan et al., 2002; Sundal et al., 2004; Breitner et al., 2010; El Afifi et al., 2006). It is well known that longshore currents generated by approaching breaking waves, transport sands particularly black fine-grained to Gaza Strip`s Coastline from Nile Delta. These currents appear to affect the transport of sediment more strongly than other mechanisms. Its transportation northward along the Mediterranean coast results from larger waves approaching from the WSW and SW than those from the WNW and NW (Zviely et al., 2007; Ubeid, 2011).

4. CONCLUSION

This study provides the first quantitative assessment of radon release and its parent nuclide (^{226}Ra) activity concentration in surface sands along the Gaza Strip beach. The objectives were to find the distributions of radon exhalation rates and radium concentrations, potentially contaminating surface sands beach in Gaza Strip. A second goal was to correlate these data with grain-size distribution of beach sand in the study area.

The sand beach of Gaza Strip is characterized by light yellow color and are composed of high percentage of quartz and around 1% of accessory minerals with dark color. The predominant grain-size distributed on the beach of Gaza Strip was medium-grained sand, and the result shows fining trend toward the north direction.

The radium concentration in beach sands of the study area varied from 0.56 to 8.46 Bq/kg, with an average value of 1.66 Bq/kg.

The activity concentration values increase towards north direction of the study area, suggesting positive correlation with the decreasing grain-size of the sediments. The highest activity concentration values were found in the Gaza and North Governorates, and they were above the standard international limits. On the other hand, the Rafah, Khan Younis and Middle Governorates recorded the lower concentration levels, below the standard international limits. Consequently, the latter ones must be preferred as favorable recreation place for people, and safe sources for construction purposes.

It cannot be excluded that the source of the pollution by radon activity in the Gaza and North Governorate and in some observation sites in Rafah and Khan Younis depends on untreated wastewater discharged in the beach. However, it is well assessed now that the contamination by radon activity in the Gaza and North Governorate is positively associated with black fine-grained sediments which were carried by longshore currents generated by approaching breaking waves.

This study could open a wide range of research on the impact of untreated wastewater on the increasing of the activity concentration in the sediments of Gaza Strip.

ACKNOWLEDGEMENTS - The authors would like to thank the editor for the efforts in publishing this article and the reviewers M. Voltaggio and P. Tuccimei for the critical revision and for their valuable comments that greatly improved the manuscript.

REFERENCES

Abed A., Al Weshahy S., 1999. Geology of Palestine. Palestinian Hydrogeological Group, Palestine, Jerusalem, pp. 461.

Aish A.M., Batelaan O., De Smedt F., 2009. Distribution recharge estimation for groundwater modeling using wetspass model, case study - Gaza Strip, Palestine. The Arabian Journal for Science and Engineering 35, 155-163.

Barillon R., Özgümüs A., Chambaudet A., 2005. Direct recoil radon emanation from crystalline phases. Influence of moisture content. Geochimica et Cosmochimica Acta 69, 2735-2744.

Baykara O., Dogru M., 2006. Measurements of radon and uranium concentration in water and soil samples from East Anatolian Active Fault Systems, Turkey. Radiation Measurements 41, 362-367.

Baykara O., Dogrua M., Inceozb M., Aksoyb E., 2005. Measurements of radon emanation from soil samples in triple-junction of North and East Anatolian active faults systems in Turkey. Radiation Measurements 39, 209-212.

Blott S.J., Pye K., 2001. Gradistat: a grain size distribution and statistics package for analysis of unconsolidated sediments. Earth Surface Processes and Landforms 26, 1237-1248.

Breitner D., Arvela H., Hellmuth K.-H., Renvall T., 2010. Effect of moisture content on emanation at different grain size fractions e A pilot study on granitic esker sand sample. Journal of Environmental Radioactivity 101, 1002-1006.

Carranza-Edwards A., Kasper-Zubillaga J.J., Rosales-Hoz L., Morales-de la Garaza E.A., Cruz, R.L.S., 2009. Beach sand and composition and provenance in a sector of the southwestern Mexican Pacific. Revista Mexicana de Ciencias Geologicas 26, 433-447.

Carranza-Edwards A., 2001. Grain size and sorting in modern beach sands. Journal of Coastal Research 17, 38-52.

Chen J., 2005. A Review of radon doses, Radiation Protection Bureau. Health Canada Radiation Protection 22, 27-31.

Darby S., Hill D., Auvinen A., Barros-Dios J.M., Baysson H., Bochicchio F., Deo H., Falk R., Forastiere F., Hakama M., Heid I., Kreienbrock L., Kreuzer M., Lagarde F., Mäkeläinen I., Muirhead C., Oberaigner W., Pershagen G., Ruano-Ravina A., Ruosteenoja E., Rosario A.S., Tirmarche M., Tomásek L., Whitley E., Wichmann H.E., Doll R., 2004. Radon in homes and risk of lung cancer: collaborative analysis of individual data from 13 European case-control studies. British Medical Journal. http://dx.doi.org/10.1136/bmj.38308.477650.63.

El Afifi E.M., Hilal M.A., Khalifa S.M., Aly H.F., 2006. Evaluation of U, Th, K and emanated radon in some NORM and TENORM samples. Radiation Measurements 41, 627-633.

Filippidis A. Misaelides P, Clouvas A., Godelitsas A., Nikolaos Barbayiannis N., Anousis I., 1997. Mineral, chemical and radiological investigation of a black sand at Touzla Cape, near Thessaloniki, Greece. Environmental Geochemistry and Health 19, 83-88.

Folk R.L., Ward W.C., 1957. Brazos River bar: a study in the significance of grain size parameters. Journal of Sedimentary Petrology 27, 3-26.

Guo Q., Cheng J., 2005. Indoor thoron and radon concentrations in Zhuhai, China. Journal of Nuclear Science and Technology 42, 588-591.

Hassan N.M., Hosoda M., Ishikawa T., Sorimachi A., Sahoo S.K., Tokonami S., Fukushi M., 2009. Radon migration process and its influence factors; review. Japanese Journal of Health Physics 44, 218-231.

Immé G., Catalano R., Mangano G., Morelli D., 2014. Radon exhalation measurements for environmental and geophysics study. Radiation Physics and Chemistry 95, 349-351.

Kannan V., Rajan M.P., Iyengar M.A.R., Ramesh R., 2002. Distribution of natural and anthropogenic radionuclides in soil and beach sand samples of Kalpakkam (India) using hyper pure germanium (HPGe) gamma ray spectrometry. Applied Radiation and Isotopes 57, 109-119.

Katheren R.L., 1998. NORM source and their origin. Applied Radiation and Isotopes 49, 149-168.

Krewski D., Lubin J.H., Zielinski J.M., Alavanja M., Catalan, V.S., Field R.W., Klotz J.B., L_etourneau E.G., Lynch C.F., Lyon J.I., Sandler D.P., Schoenberg J.B., Steck D.J., Stolwijk J.A., Weinberg C., Wilcox H.B., 2005. Residential radon and risk of lung cancer; a combined analysis of 7 North American case-control studies. Epidemiol 16, 137-145.

Lubin J.H., Wang Z.Y., Boice J.D., Xu Z.Y., Blot W.J., De Wang L., Kleinerman R.A., 2004. Risk of lung cancer and residential radon in China: pooled results of two studies. International Journal of Cancer 109, 132-137.

Markkanen M., Arvela H., 1992. Radon emanation from soils. Radiation Protection Dosimetry 45, 269-272.

Menetrez M.Y., Mosley R.B., 1996. Evaluation of radon emanation from soil withvarying moisture content in a soil chamber. Environment International 22, 447-453.

Nazaroff W.W., 1992. Radon transport from soil to air. Reviews of Geophysics 30, 137-160.

NCRP (National Council for Radiation Protection and Measurements), 1987. Report no. 93.

Rahman S., Mati N., Matiullah, Ghauri B., 2007. Radon exhalation rate from the soil, sand and brick samples collected from NWFP and FATA, Pakistan. Radiation Protection Dosimetry 124, 392-399.

Saad A.F., Abdallah R.M., Hussein N.A., 2013. Radon exhalation from Libyan soil samples measured with the SSNTD technique. Applied Radiation and Isotopes 72, 163-168.

Scholten L.C., Timmermans C.W.M., 1996. Natural radioactivity in phosphate fertilizers. Fertilizer Research 43, 103-107.

Soghreah, 1996. Gaza Port - Part II, layout report, Section II, Site conditions study.

Sroor A., El-Bahi S.M., Ahmed F., Abdel-Haleem A.S., 2001. Natural radioactivity and radon exhalation rate of soil in southern Egypt. Applied Radiation and Isotopes 55, 873-879.

Shoqwara F., Dwaikat N., Saffarini G., 2013. Measurement of radon exhalation rate from building materials. Research & Reviews: Journal of Physics 2, 10-19.

Shweikani R., Giaddui T.G., Durrani S.A., 1995. The effect of soil parameters on the radon concentration values in the environment. Radiation Measurements 25, 581-584.

Sundal A.V., Henriksen H., Lauitzen S.E., Soldal O., Strand T., Valen V., 2004. Geological and geochemical factors affecting radon concentrations in dwellings located on permeable glacial sediments - a case study from Kinasarvik, Norway. Environmental Geology 45, 843-858.

Ubeid K.F., 2010. Marine lithofacies and depositional zones analysis along coastal ridge in Gaza Strip, Palestine. Journal of Geography and Geology 2, 68-76.

Ubeid K.F., 2011. Sand Characteristics and Beach Profiles of the Coast of Gaza Strip, Palestine. Serie Correlacion Geologica 27, 121-132.

Ubeid K.F., Albatta A. 2014. Sand dunes of the Gaza Strip (southwestern Palestine): morphology, textural characteristics and associated environmental impacts. Earth Sciences Research Journal, 18, 131-142.

UNSCEAR (United Nations Scientific Committee on the Effects of Atomic Radiation), 1988. Exposure from natural sources of radiation. In: Source and Effects of Ionizing Radiation. Scientific Committee on the Effects of Atomic Radiation, United Nations, New York.

UNSCEAR (United Nations Scientific Committee on the Effects of Atomic Radiation), 2000. Sources and Effects of Ionizing Radiation, United Nations Scientific Committee on the Effects of Atomic Radiation. Report to General Assembly with Scientific Annexes, United Nations, New York.

USEPA (United States Environmental Protection Agency), 2003. EPA's Assessment of Risks from Radon in Homes, EPA 402-R-03-003. Office of Radiation and Indoor Air, United States Environmental Protection Agency, Washington.

Zviely D., Kit E., Klein M., 2007. Longshore sand transport estimates along the Mediterranean coast of Israel in the Holocene. Marine Geology 238, 61-73.